# Engineering and Applied Science Research

# Succinic acid production from lignin by photo-oxidation

Manmard Suttipornphaisalkul[1], Phillip Wright[2] and Khanita Kamwilaisak*[1, 3]

[1]Department of Chemical Engineering, Faculty of Engineering, Khon Kaen University, Khon Kaen 40002, Thailand
[2]Faculty of Science, Agriculture and Engineering, Newcastle University, NE1 7RU, United Kingdom
[3]Sustainable infrastructure Research and Development Center, Khon Kaen University, Khon Kaen 40002, Thailand

## Abstract

Lignin is one of three components that make up wood, and it is the most recalcitrant among these compounds due to its highly degradation-resistant phenolic polymer structure. Lignin is composed of carbon, oxygen and hydrogen, which has the potential to be a feedstock for biofuels and biorefining processes. In this work, lignin was depolymerized to produce succinic and acetic acids via a photocatalytic reaction. $TiO_2$ and $H_2O_2$ under UV-light were used as a photocatalyst and photocatalyst promoter, respectively. The effect of $TiO_2$ and $H_2O_2$ dosage, solution pH and reaction time on % yield of dicarboxylic acid was determined. Optimization of reaction conditions was done with response surface methodology using a Box-Behnken design. It was found that the maximum %yield of succinic acid (7.8%) was at a reaction time of 24 h, a 2.37 g/l of $TiO_2$ dosage and 25.45 µl of $H_2O_2$ dosage and pH 7.0. The predicted dicarboxylic acid yield using was accurate with $R^2$=91.8%. This would be an alternative way to produce high-value fine chemicals from lignin.

## 1. Introduction

Lignocellulose is abundant in plant biomass. It consists of three main components-cellulose (40-50%), hemicellulose (24-35%), and lignin (18-35%) [1]. Their relative composition varies depending on species, age and cultivation location of the biomass sources [2]. Cellulose is a long-chain polymer composed of numerous D-glucose units connected by hydrogen bonds. The length of the chain affects its physical properties such as rigidity, crystallinity and solubility in water. Therefore decomposition of cellulose needs to be done under harsh conditions. Hemicellulose is a shorter branch polymer that acts as a linkage between cellulose and lignin [3]. Cellulose and hemicellulose are used as feedstocks for alternative fuels and chemical products [2]. Lignin is the largest renewable source of aromatics [1, 3-4] with 3-dimensional amorphous polymers randomly composed of 3 phenylpropane monomer units, guaiacyl (G), syringyl (S), p-hydroxyphenyl (H) [5-7]. The structure of lignin depends on the species and biomass sources [8]. Lignin is a waste by-product of biorefining and pulping. This material is currently burned as a low-value fuel to provide heat and power for other processes [3-4]. It has been reported that lignin can be utilised as an absorbent. Due to its rich aromatic structure, lignin has outstanding properties for petroleum-based chemical substitution [9-10]. High-value fine chemicals and fuel can be produced from sustainable biomass materials. This has received increased attention, and some success has been achieved.

Dicarboxylic acids (DCAs) and their derivatives are one of the crucial groups of fine products used in the chemical, pharmaceutical, food and fuel industries. They can be produced from lignin by breaking down its chemical structure [1, 7, 9, 11]. Production of dicarboxylic acid from fossil-derived sources requires decomposition of C-H or C-C bonds and formation of C-O bonds via oxygen atom insertion. By contrast, biomass has a sufficient amount of oxygen atoms with abundant C-O bonds; therefore, the production of acid from biomass resources is more economically feasible and environmentally friendly [8].

Depolymerization of lignin can be done by various biological processes using enzymes; however, long retention time is required [12]. Hydrothermal wet oxidation for lignin depolymerization has to be done under severe conditions [13]. Among the various processes, advanced oxidation process (AOPs) are the most attractive. AOPs, describe processes which employ highly reactive chemical oxidants and hydroxyl radicals (OH·) for oxidation [9, 14]. Oxidation of lignin and lignin monomers has been reported using various AOPs. Hydrothermal processes are AOPs that require additional energy input for oxidation reactions in a high-temperature fluid with short reaction times. However, the disadvantage of this process is low selectivity in chemical production and char formation [15-16]. Additionally, Fenton's reaction can occur. It is associated with hydrogen

peroxide and ferrous salt to generate OH˙. The reaction needs to be done at relatively low pH values in an aqueous medium [9, 11, 17]. In the presence of hydrogen peroxide, photooxidation and photocatalysis can easily form OH˙ via UV radiation [12, 18-22]. Among the semiconductors, titanium dioxide has considerable potential for photocatalytic oxidation of lignin because of its non-toxic and stable properties in both acidic and alkaline environments [23]. The use of $TiO_2$ for the degradation of toxic pollutants and lignin has been reported [12, 20, 24]. Investigating the interactions between process parameters such as reaction time, $TiO_2$ dosage and hydrogen peroxide dosage and their impact % yield of dicarboxylic acid from lignin degradation under $TiO_2$/UV systems has been done using response surface methodology (RSM).

RSM is a statistical tool used to optimize the parameters for desirable responses and generate mathematical models for predicting process responses to changes in parameter values. There are three experimental design methods commonly used for RSM. Full factorial design (FFD) is an impractical method due to a large number of required experiments. Central composite design (CCD) requires a large number of experiments, which include parameter values over a wide practical range of benefits. Box-Behnken design (BBD) is commonly used to design a quadratic response surface for three factors that employ three levels of each process parameter, and it requires fewer experiments [25-27]. Evaluating optimal conditions for lignin degradation under a $TiO_2$/UV system can be adapted for a manufacturing process producing dicarboxylic acid. RSM was applied to experimental data using the statistical software package, Minitab.

In the present work, Kraft lignin photocatalytic oxidation using $TiO_2$ as a catalyst in the presence of hydrogen peroxide was investigated. This was done to explore the effect of solution pH, reaction time, and hydrogen peroxide and $TiO_2$ dosage on the yield of dicarboxylic acid. To further understand lignin depolymerization, the reaction mechanism was explored via GC-MS to guide scaling up the process for industrial use. To our best knowledge, no such work has been done considering the amount of succinic acid as an intermediate product from depolymerization of Kraft lignin. The aim of this work is to find an alternative way to produce fine chemicals from renewable carbon resources with mild processes that do not require microorganisms. The optimum reaction conditions for high % yield of succinic acid from depolymerized Kraft lignin were determined.

## 2. Materials and methods

### 2.1 Materials

Kraft lignin (Aldrich, US), sulfuric acid (RCI Labscan, Thailand), sodium hydroxide (RCI Labscan, Thailand), acetonitrile (Merck, Germany), succinic acid (analytical grade, Ajax Finechem, Australia), acetic acid (analytical grade, QReC, New Zealand), hydrogen peroxide (30%, Merck, Germany) and titanium dioxide (Degussa P25 commercial-grade, $TiO_2$, Merck, Germany) were used in the current study.

### 2.2 Decomposition of lignin

All experiments were performed in 25 ml flasks containing 10 ml of a lignin solution, $H_2O_2$ and $TiO_2$. The pH of a 1,000 mg/l lignin solution was adjusted so that it was in the range of 5.5 – 10.3 using sodium hydroxide as an alkali

or sulfuric acid as an acid. The reactions were carried out under vigorous stirring at 250 rpm in a heated glycerol bath on a heated stirrer at 50 °C inside a UV box. After the desired reaction time, the flask was removed from the glycerol bath, and $TiO_2$ was immediately separated using a 0.22 μm nylon filter. A schematic of the experimental setup used in this study is shown in Figure 1.
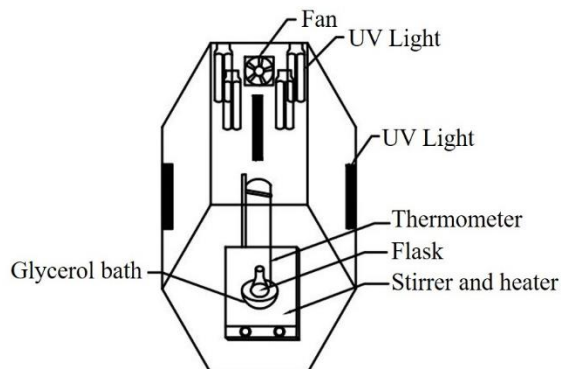


**Figure 1** Schematic of the experimental setup used in this study
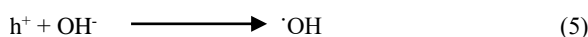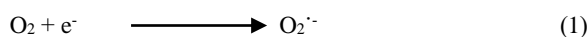
### 2.3 Product analysis

The resulting solution was filtered through a 0.22 μm filter and analyzed using high-performance liquid chromatography (HPLC) in a C-18 column (Restek Ultra AQ) equipped with a UV-Vis detector (240 nm) for identification and quantification of dicarboxylic acid. The yield of the dicarboxylic acid was defined based on DCA and lignin concentrations as follows:

$$\%yield = \frac{dicarboxylic\ acid\ concentration(g/L)}{initial\ concentration\ of\ lignin(g/L)} \times 100$$

## 3. Results

After the reaction, the solution was filtered through a 0.22 μm nylon filter. Then the filtrate was analyzed by means of HPLC using a C-18 column (Restek Ultra AQ). The predominant products of lignin oxidation were acetic and succinic acids.

The photocatalytic oxidation mechanism of titanium dioxide ($TiO_2$) could be explained by equations 1-5 When $TiO_2$ is illuminated with greater energy than its bandgap (3.2eV), electrons ($e^-$) will move from the valence band to conduction band, leaving a hole ($h^+$) in the valence band. In the valence band, the evacuated electrons interact with oxygen atoms producing superoxide radicals ($O_2^{\cdot-}$). Meanwhile, the hole in the valence band interacts with water molecules producing hydroxyl radicals (OH˙). These radicals will decompose lignin molecules [28-29] as follows:

$$O_2 + e^- \longrightarrow O_2^{\cdot-} \tag{1}$$

$$O_2^{\cdot-} + H^+ \longrightarrow HO_2^{\cdot} \tag{2}$$

$$2HO_2^{\cdot} \longrightarrow H_2O_2 + O_2 \tag{3}$$

$$H_2O_2 + e^- \longrightarrow HO^{\cdot} + OH^- \tag{4}$$
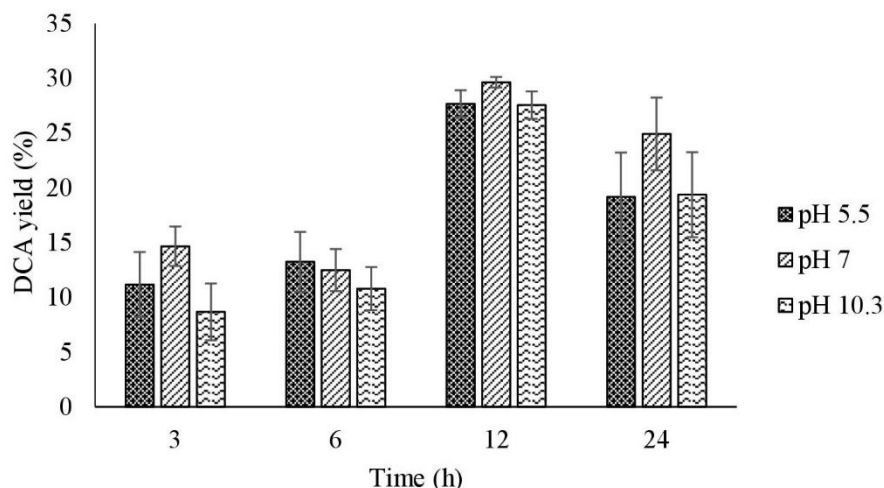
$$h^+ + OH^- \longrightarrow {}^{\cdot}OH \tag{5}$$

**Figure 2** Influence of pH and reaction time on % yield of dicarboxylic acid from lignin oxidation in a $TiO_2/H_2O_2$ system. Reaction conditions: lignin 1 g/l, $H_2O_2$ 10 µl.
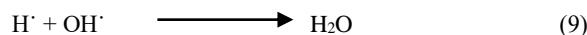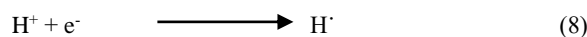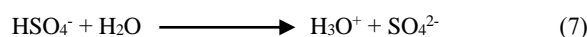
*3.1 Influence of pH solution and reaction time*

Surface properties of the photocatalyst play an vital role in photocatalysis. Since the reaction takes place on the photocatalyst surface, adsorption and desorption are strongly influenced by the acid-base equilibrium [30]. In order to investigate the efficacy of the $TiO_2/H_2O_2$ system, the effect of reaction time and pH of the solution on lignin oxidation and production of dicarboxylic acid was investigated by varying reaction time at 3, 6, 12 and 24 h and pH of the solution from 5.5 to 10.3.

Reaction conditions included lignin at 1 g/l and $H_2O_2$ at 10 µl. As Figure 2 shows, varying pH of solutions significantly affected the % yield of dicarboxylic acid. Under all solution pH values, the increase in reaction time from 3 h to 12 h significantly increased the quantity of DCA, especially from 6 h to 12 h. During this time, the yield of DCA increased more than twofold from 13. 2, 12. 5 and 10.8% to 27.7, 29.6 and 27.5%. After 24 h of reaction, the yields of DCA dropped to 19.1, 14. 9 and 19. 4% , respectively.

During the first 6 h of the degradation process, lignin began to break down from high molecular weight into lower molecular weight aromatic compounds, resulting in low yields of DCA. [6, 11, 15] (See Section 3.4 for more details).

A number of factors could account for the lower %yield of DCA under acidic conditions. The solution pH values were adjusted by the addition of sulfuric acid ($H_2SO_4$). When sulfuric acid is dissolved in water, the dissociation process starts with the generation of hydronium and hydrogen sulfate ions. Then hydrogen sulphate ions react with water molecules producing more hydronium and sulphate ions following equations (6-7). Titanium dioxide can adsorb $SO_4^{2-}$ via van der Waals forces and hydrogen bonds. Active sites on the surface may be occupied by $SO_4^{2-}$, which has the effect of reducing the photocatalytic activity [21]. Moreover, titanium dioxide tends to agglomerate into bigger particles under acidic conditions. Consequently, photo- absorption would be diminished, and fewer $OH^·$ produced from $TiO_2$ for lignin oxidation [31]. Additionally, the presence of excess $H^+$ can interact with free electrons in the valence band of $TiO_2$ to form $H^·$. Then $H^·$ can react with $OH^·$ converting the radicals back to water molecules as equations (8-9) [29, 32].

$$H_2SO_4 + H_2O \longrightarrow H_3O^+ + HSO_4^- \qquad (6)$$

$$HSO_4^- + H_2O \longrightarrow H_3O^+ + SO_4^{2-} \qquad (7)$$

$$H^+ + e^- \longrightarrow H^· \qquad (8)$$

$$H^· + OH^· \longrightarrow H_2O \qquad (9)$$

In an alkaline solution, it was widely reported that the photocatalytic process in the presence of hydrogen peroxide at an alkaline pH ( pH >7) could obstruct hydroxyl radical production because hydrogen peroxide rapidly decomposes to water and oxygen at these pH values [33-35]. Therefore the % yield of succinic and acetic acids from depolymerization of lignin is slightly lower than at other pH values under alkaline conditions.

Further, the point of zero charges ( Pzc) of $TiO_2$ is at a pH of 6.25 - 6.8. When the pH of a solution is decreased to a value lower than Pzc, the surface of $TiO_2$ is more positively charged and vice versa. The surface of $TiO_2$ is neutral when the pH of the solution is equal to the Pzc [30-32] . Oxidized lignin consists of low molecular weight aromatic compounds such as quinone and dicarboxylic acid, which are nonpolar to slightly polar. Adjusting the pH of the solution so that it deviates from the Pzc would limit adsorption of the reactant. These results indicate that oxidation of lignin at a neutral pH will achieve the highest %yield of DCA.

*3.2 Influence of hydrogen peroxide*

The depolymerization of lignin by $TiO_2$ as a photocatalyst with and without hydrogen peroxide was conducted. The results are shown in Figure 3. After 24 h of reaction time, the %yield of DCA reached its maximum, 20% to 29%, when an increasing amount of $H_2O_2$ from 0 to 10 µl. This increased the concentration of hydroxyl radicals ($OH^·$) with restricted electron- hole pair recombination [30]. In contrast, an increasing amount of $H_2O_2$ from 30 to 50 µl, resulted in a %yield of DCA that was significantly reduced from 29% to 18%. It dropped to 1% with 50 ul of $H_2O_2$, and succinic acid was not detected. This can be explained as $H_2O_2$ dissociated into $OH^-$ and $OH^·$ radicals when exposed to UV-light following equations (10-12). Additionally, $O_2^{·-}$ and $OH^·$ radicals were also generated by the $TiO_2/UV$ mechanism. Excess radicals caused severe oxidation of the
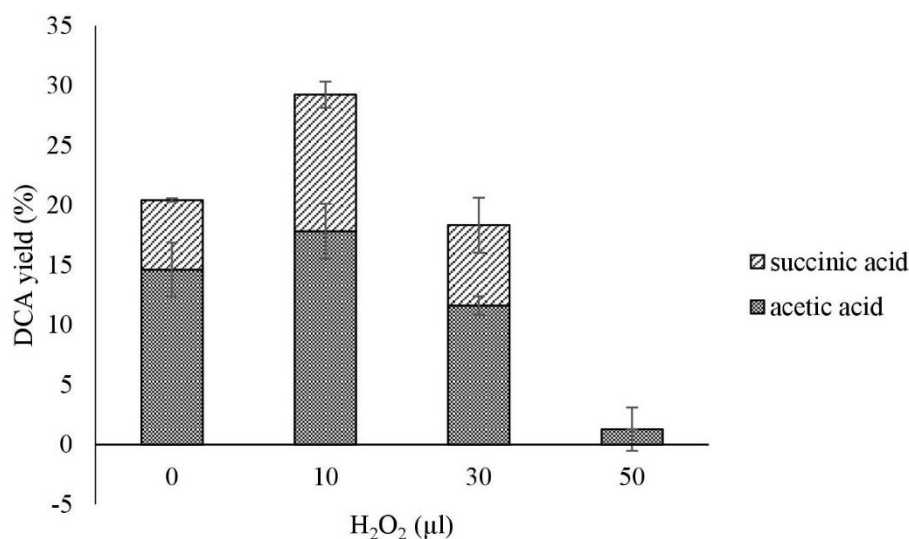
**Figure 3** Influence of hydrogen peroxide dosage on %yield of dicarboxylic acid from lignin oxidation in $TiO_2/H_2O_2$ systems. Reaction conditions: lignin 1 g/l, $TiO_2$ 2 g/l and 24h.
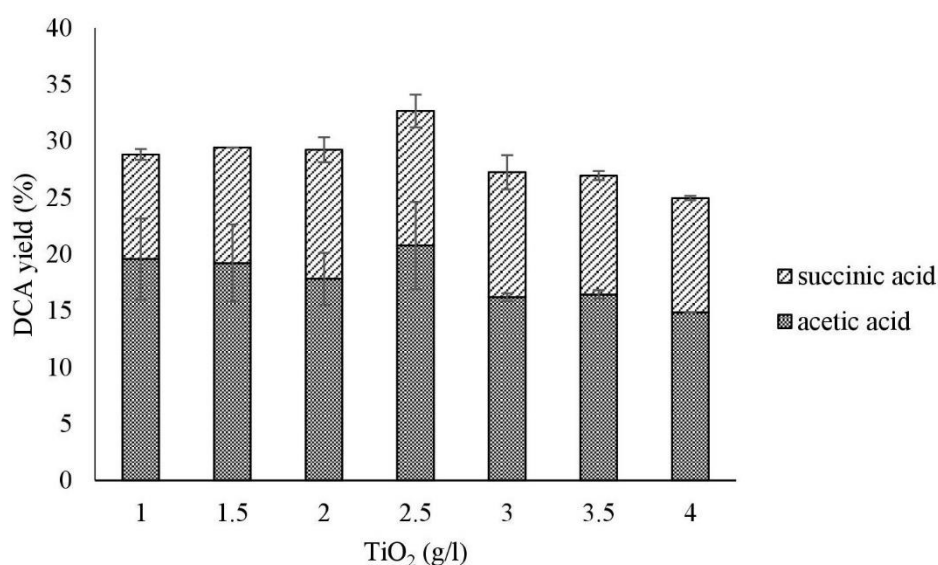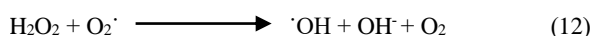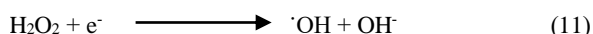


**Figure 4** Influence of $TiO_2$ dosage on % yield of dicarboxylic acid from lignin oxidation in $TiO_2/H_2O_2$ systems. Reaction conditions: lignin 1 g/l, $TiO_2$ 2 g/l and 24h.
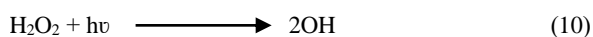
target compound to smaller molecules and ultimately to complete mineralization into carbon dioxide and water.

$$H_2O_2 + h\upsilon \longrightarrow 2OH \qquad (10)$$

$$H_2O_2 + e^- \longrightarrow {}^\cdot OH + OH^- \qquad (11)$$

$$H_2O_2 + O_2{}^\cdot \longrightarrow {}^\cdot OH + OH^- + O_2 \qquad (12)$$

It has been reported that the amount of H2O2 supplied influences the conversion of lignin monomers to dicarboxylic acid in a $CuFeS_2/H_2O_2$ system and % yield of DCA decreased with excess $H_2O_2$ [6]. Moreover, $H_2O_2$ supplied over the optimum condition for best %yield with a four- carbon DCA sharply dropped, indicating further product oxidation to $CO_2$ and $H_2O$ [16].

In the lignin degradation process, acetic acid is produced from breaking the bonds between phenolic and functional groups, of which there are many in lignin molecules.

Succinic acid is created by depolymerizing the benzene ring, which requires several steps. This is the reason why the yield of acetic acid is higher than succinic acid [12, 36-37] (see Section 3.4 for further details).

*3.3 Influence of titanium dioxide*

Experiments were carried out by varying $TiO_2$ dosages from 1 g/l to 4 g/l to study the % yield of DCA from lignin oxidation under UV irradiation in the presence of $H_2O_2$ at a neutral pH. This was done to determine the effect of $TiO_2$ loading. The result is shown in Figure 4. As the amount of catalyst increased, the % yield of DCA slightly increased from 28.8% to 32.6%. When the catalyst loading increased from 1 g/l to 2.5 g/l, it decreased, DCA yield dropped to 25%. This can be described as follows. When the amount of $TiO_2$ was increased, the number of active sites on its surface increased. Therefore, more radicals were generated in the system, resulting in greater %yields. However, further

**Table 1** Factors and levels of the experimental study

| Factors | Levels | | |
| --- | --- | --- | --- |
| | Low (-1) | Middle (0) | High (1) |
| $X_1$ : Reaction time (hr) | 6 | 15 | 24 |
| $X_2$ : TiO$_2$ Dosage (g/l) | 1 | 2 | 3 |
| $X_3$ : H$_2$O$_2$ Dosage (μl) | 0 | 15 | 30 |

increases in the amount of TiO$_2$ caused the %yield of DCA to decrease. This results from higher turbidity of the solution from the more massive amounts of TiO$_2$ limiting the irradiation of UV light [38].

*3.4 Possible reaction mechanism*

The possible reaction mechanism for dicarboxylic acid productions has been proposed by Kamwilaisak and Wright [12]. They explained the role of TiO$_2$/UV on lignin depolymerization into dicarboxylic acid. Exposure of the samples with TiO$_2$ to UV light generated OH. radicals, with H$_2$O$_2$ acting in a synergistic reaction.

That produced a massive amount of OH$^.$, The most reactive radicals for dicarboxylic acid production disrupted the linkages between phenolic monomers and rings. Starting with cleavage between rings (C-C and ether bonds), low molecular weight phenolic compound such as catechol, phenolic ketone, phenolic acid and quinone were produced. Then ring disruption of these molecules occurred, producing malonic acid and its subsequent oxidation into smaller acids, i.e., acetic and succinic acids. This can affirm that abundant phenolic biomass can be decomposed in an environmental friendly mild reaction [7, 12, 24, 37, 39].

*3.5 Optimization of the process for succinic acid production*

According to the US Department of Energy (DOE), succinic acid is one of the top 12 most valuable biochemicals. Succinic acid is widely used in many industrial processes, including the production of biodegradable plastics, pharmaceuticals and food. One of the most impactful applications of succinic acid is in the production of biodegradable plastics. Currently, most production of succinic acid is by microbial fermentation of sugar [40-42]. In the present work, succinic acid was produced from lignin under mild conditions that employed no microbial action. Optimization of process conditions was conducted. Process parameters were varied to identify the optimal conditions for succinic acid production and to investigate the interactions between these parameters. Reaction time, TiO$_2$ dosage and hydrogen peroxide dosage were modelled using a Box Behnken Design (BBD) under RSM. The response surface regression to fit the full quadratic expression is given by equation (13).

$$Y = \beta_0 + \beta_1 X_1 + \beta_2 X_2 + \beta_3 X_3 + \beta_4 X_1{}^2 + \beta_5 X_2{}^2 + \beta_6 X_3{}^2 + \beta_7 X_1 X_2 + \beta_8 X_1 X_3 + \beta_9 X_2 X_3 \pm \varepsilon \qquad (13)$$

where:    Y is the predicted response, % yield of succinic acid
          $X_i$ are dependent variables: $X_1$, $X_2$ and $X_3$ reaction time, TiO$_2$ dosage and H$_2$O$_2$ dosage, respectively

$\beta_i$ are regression coefficients
$\varepsilon$ is an error term

RSM was applied to the experimental data using Minitab. The levels of the three factors, reaction time, TiO$_2$ dosage and hydrogen peroxide dosage, were chosen based on data summarized in Table 1.

Three factors at three levels in a Box Behnken response surface design with two replicates were used for optimizing process condition and for investigating the interaction between factors on % yield of succinic acid along with experimental and predicted values shown in Table 2. The experiments were performed in random order to avoid bias.

The predicted equation for % yield of succinic acid was obtained by quadratic model fitting as presented in Equation (14. ANOVA tests of regression coefficients with confidence levels of 95% are shown in Table 3.

Considering p-values < 0.05 as significant for the response [25, 43], the response function predictions agreed well with the experimental data with $R^2 = 91.82\%$. The value of the adjusted $R^2$, discarding the non-significant factors, is $R^2$adj = 88.14%. The $R^2$adj value is less than the $R^2$ from the full quadratic equation, indicating that the full quadratic equation is slightly more precise for prediction of % yield of succinic acid. Figure 5 presents a random scatter plot of actual values and the predicted results of %yield of succinic acid. It can be observed that the experimental data was scattered along the prediction line within ± 10%, demonstrating a good correlation between the two data sources.

Y (%yield of succinic acid) = -4.236+0.103$X_1$+2.924$X_2$+ 0.444$X_3$+0.004$X_1{}^2$-0.618 $X_2{}^2$-0.005$X_3{}^2$+0.008$X_1X_2$- 0.008$X_1X_3$-0.007$X_2X_3$                                        (14)

According to initial assumptions of data analysis using the ANOVA method, the experimental data must be normally distributed (α=0.05). From Figure 6, residual plots for %yield of succinic acid indicated that the experimental data agree with ANOVA. An analysis of variance (ANOVA) was performed to evaluate the adequacy and suitability of the full quadratic model with the Fisher variance ratio, F-value. The calculated F-value of the variable was compared with the F-critical value. An F-value with a magnitude greater than or equal to F-critical indicates that the variable has an effect on %yield of succinic acid. The critical F-value for lack-of-fit, F(0.05,3,17) is 3.1 and actual F-value of lack-of-fit is 1.15. This indicates that the errors in the experiments are insignificant, suggesting that full quadratic equation is valid at a 95% statistical confidence level (shown in Table 4) [27].

*3.5.1 The interaction effects*

A contour plot was obtained by plotting the %yield of succinic acid against functions of two variables while

**Table 2** Experimental %yield of succinic acid and predicted values obtained by BBD

| Run | Factors and Levels | | | Response (%yield of succinic acid) | |
|---|---|---|---|---|---|
| | -1 | 0 | 1 | Experimental | Predicted |
| 1 | 6 | 1 | 15 | 4.09 | 3.67 |
| 2 | 24 | 2 | 0 | 4.91 | 4.34 |
| 3 | 15 | 2 | 15 | 7.36 | 5.50 |
| 4 | 15 | 2 | 15 | 6.62 | 5.50 |
| 5 | 24 | 2 | 0 | 4.18 | 4.34 |
| 6 | 6 | 1 | 15 | 3.73 | 3.67 |
| 7 | 24 | 2 | 30 | 7.11 | 7.46 |
| 8 | 6 | 3 | 15 | 4.50 | 4.47 |
| 9 | 24 | 2 | 30 | 7.22 | 7.46 |
| 10 | 6 | 2 | 0 | 0.57 | 0.00 |
| 11 | 15 | 3 | 30 | 7.81 | 6.75 |
| 12 | 24 | 1 | 15 | 6.88 | 5.83 |
| 13 | 6 | 3 | 15 | 3.79 | 4.47 |
| 14 | 24 | 3 | 15 | 6.78 | 6.90 |
| 15 | 15 | 3 | 0 | 2.07 | 1.79 |
| 16 | 24 | 3 | 15 | 6.54 | 6.90 |
| 17 | 15 | 2 | 15 | 5.53 | 5.50 |
| 18 | 15 | 3 | 0 | 1.58 | 1.79 |
| 19 | 15 | 2 | 15 | 4.14 | 5.50 |
| 20 | 6 | 2 | 30 | 7.32 | 7.20 |
| 21 | 15 | 2 | 15 | 4.26 | 5.50 |
| 22 | 15 | 3 | 30 | 6.75 | 6.75 |
| 23 | 15 | 2 | 15 | 5.11 | 5.50 |
| 24 | 15 | 1 | 0 | 0.21 | 0.65 |
| 25 | 15 | 1 | 0 | 0.03 | 0.65 |
| 26 | 15 | 1 | 30 | 6.32 | 6.01 |
| 27 | 6 | 2 | 30 | 6.67 | 7.20 |
| 28 | 6 | 2 | 0 | 0.00 | 0.00 |
| 29 | 15 | 1 | 30 | 5.64 | 6.01 |
| 30 | 24 | 1 | 15 | 5.42 | 5.83 |

**Table 3** %yield regression coefficients obtained using the least square of error technique

| Term | Coefficient | p-value |
|---|---|---|
| Constant | -4.236 | 0.000 |
| Reaction Time, $(X_1)$ | 0.103 | 0.000 |
| $TiO_2$ Dosage, $(X_2)$ | 2.924 | 0.034 |
| $H_2O_2$ Dosage, $(X_3)$ | 0.444 | 0.000 |
| Reaction Time*Reaction Time, $(X_1^2)$ | 0.004 | 0.288 |
| $TiO_2$ Dosage* $TiO_2$ Dosage, $(X_2^2)$ | -0.618 | 0.055 |
| $H_2O_2$ Dosage* $H_2O_2$ Dosage, $(X_3^2)$ | -0.005 | 0.002 |
| Reaction Time*$TiO_2$ Dosage, $(X_1* X_2 )$ | 0.008 | 0.814 |
| Reaction Time* $H_2O$ Dosage, $(X_1* X_3)$ | -0.008 | 0.002 |
| $TiO_2$ Dosage* $H_2O_2$ Dosage, $(X_2* X_3)$ | -0.007 | 0.735 |
| $R^2$ | 91.82% | |
| $R^2$(adj) | 88.14% | |
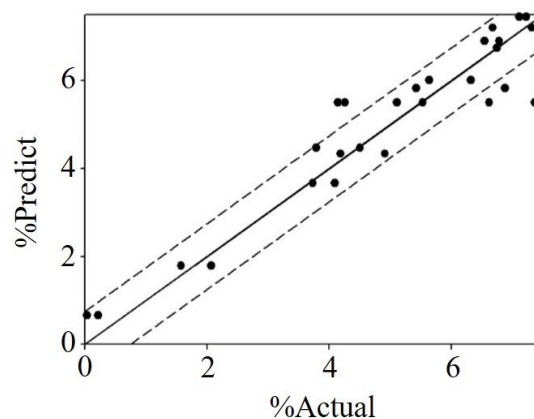


**Figure 5** Comparative plot between predicted and experimental data of %yield of succinic acid

## Residual Plots for % yield succinic acid

### a.) Normal Probability Plot



### b.) Versus Fits



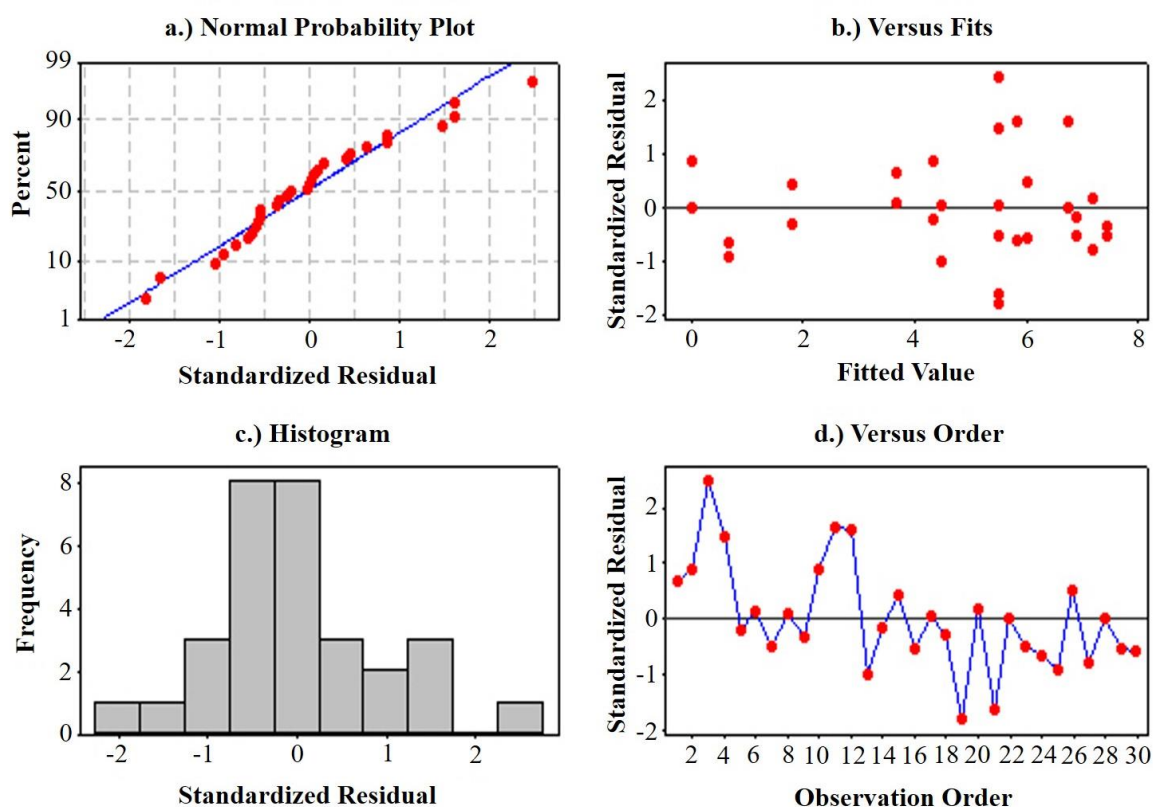### c.) Histogram



### d.) Versus Order



**Figure 6** Residual plots for %yield of succinic acid a) normal probability plot, b) versus plot, c) histogram d.) versus order

**Table 4** ANOVA results for %yield of succinic acid

| Source | DF | SS | MS | F | P | F-Critical |
|---|---|---|---|---|---|---|
| Regression | 9 | 151.97 | 16.886 | 24.94 | 0.000 | 2.39 |
| Linear | 3 | 131.142 | 43.714 | 64.56 | 0.000 | 3.1 |
| $X_1$ | 1 | 21.088 | 21.088 | 31.15 | 0.000 | 4.35 |
| $X_2$ | 1 | 3.5 | 3.5 | 5.17 | 0.034 | 4.35 |
| $X_3$ | 1 | 106.554 | 106.554 | 157.37 | 0.000 | 4.35 |
| Square | 3 | 12.358 | 4.119 | 6.08 | 0.004 | 3.1 |
| $X_1^2$ | 1 | 1.529 | 0.808 | 1.19 | 0.288 | 4.35 |
| $X_2^2$ | 1 | 2.123 | 2.821 | 4.17 | 0.055 | 4.35 |
| $X_3^2$ | 1 | 8.706 | 8.706 | 12.86 | 0.002 | 4.35 |
| Interaction | 3 | 8.47 | 2.823 | 4.17 | 0.019 | |
| $X_1 * X_2$ | 1 | 0.038 | 0.038 | 0.06 | 0.814 | 4.35 |
| $X_1 * X_3$ | 1 | 8.352 | 8.352 | 12.34 | 0.002 | 4.35 |
| $X_2 * X_3$ | 1 | 0.08 | 0.08 | 0.12 | 0.735 | 4.35 |
| Residual Error | 20 | 13.541 | 0.677 | | | |
| Lack-of-Fit | 3 | 2.28 | 0.76 | 1.15 | 0.359 | 3.1 |
| Pure-Error | 17 | 11.262 | 0.662 | | | |
| Total | 29 | 165.512 | | | | |

keeping the third variable constant at its mean value. The effects of reaction time, TiO2 dosage and H2O2 dosage on %yield of succinic acid are shown in Figure 7. With the interaction between reaction time and TiO2 dosage, the %yield of succinic acid is high when both variables at high values. Similarly, with the interaction between reaction time and H2O2 dosage, %yield of succinic acid is high when both reaction time and H2O2 concentration are high. The %yield of succinic acid is high when H2O2 dosage is high while TiO2 is in a range of 2.0 – 2.5 g/l.

As shown in Figure 8, the % yield of succinic acid increases with reaction time. Depolymerization of lignin to dicarboxylic acid could be separated into various steps, starting with decomposition into low molecular weight aromatic compounds. Then, it degrades to quinones and last breaks down to dicarboxylic acid [7, 11-12, 37]. In this pathway, more aromatics from the primary step can break down to dicarboxylic acid with longer reaction times. This result agrees with Shilpy et al.[44] who showed that with longer reaction time, more massive molecules, such as vanillic acid, break down to a smaller molecule, vanillin. Similarly, in the work of Bi et al. [6], lignin depolymerized to aromatic compounds first and then broke down to dicarboxylic acid with increasing time. This agree wells with Ma et al. [11].
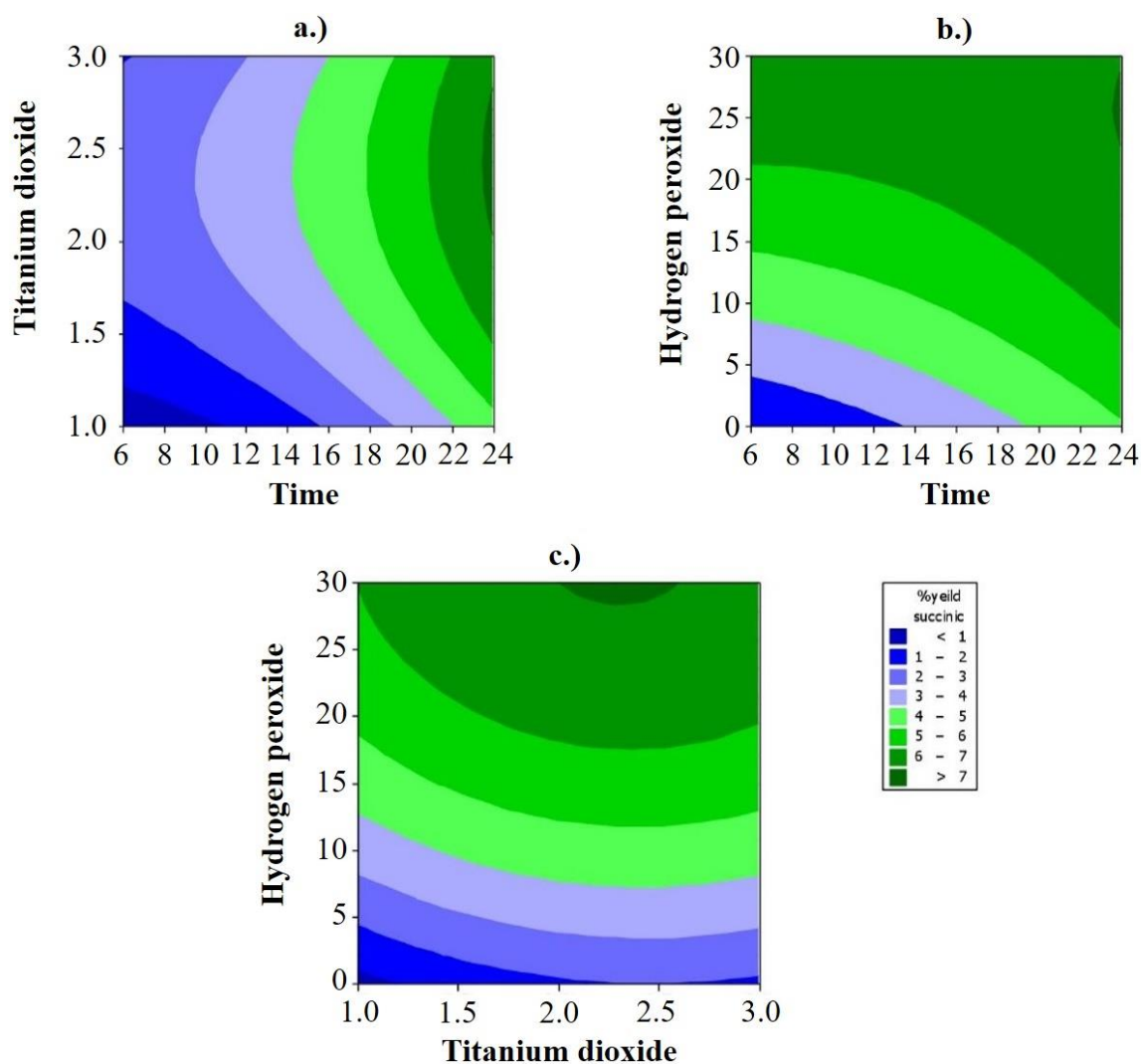
**Figure 7** Contour plot of %yield of succinic acid considering the effect of reaction time with TiO₂ vs H₂O₂ dosages. a) TiO₂ dosage vs. time, b) H₂O₂ dosage vs. time, and c) TiO₂ dosage vs. H₂O₂ dosage, for depolymerization followed by aromatic ring disruption to produce DCA
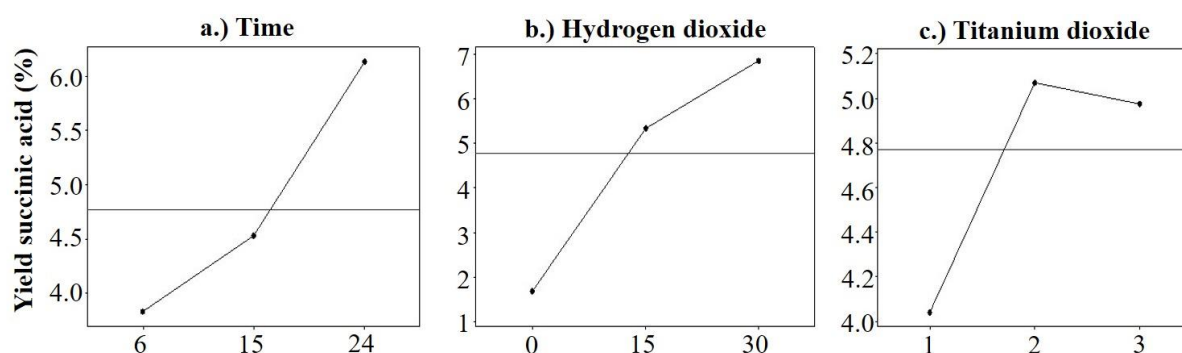


**Figure 8** Main effect plot for %yield of succinic acid. Effect of a) reaction time, b) H₂O₂ dosage, and c. TiO₂ dosage

Hydroxyl radicals are crucial in breaking down the linkages, and benzene rings in lignin molecules into dicarboxylic acid [6, 16]  as titanium dioxide dosage increased from 1 to 2 g/l, the % yield of succinic acid risen from 4% to around 5%. Under TiO₂/UV in the presence of hydrogen peroxide, hydroxyl was produced via the synergistic effect of TiO₂ and hydrogen peroxide. In contrast, when the TiO₂ dosage was increased from 2 g/l to 3g/l, the

% yield of succinic acid slightly decreased as a result of excess TiO₂, which limited hydroxyl radical production. This result agrees with Shilpy et al. [44] and Bi et al. [6], who showed that an excess of catalyst reduces substrate conversion.

Figure 9 shows that hydrogen peroxide dosage has a positive effect on the % yield of succinic acid. When hydrogen peroxide is exposed to UV light, a higher initial
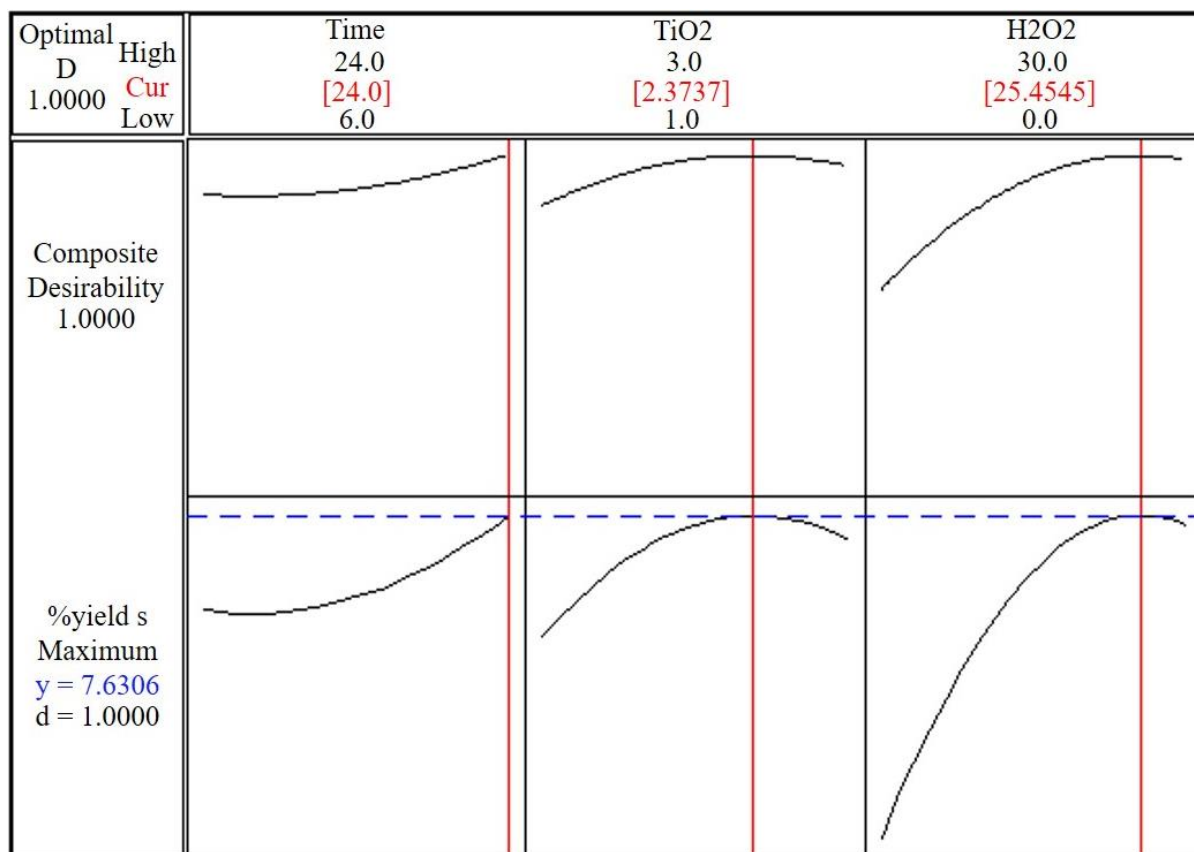
**Figure 9** diagrammatic optimization of succinic acid production from lignin depolymerization by $TiO_2$/UV in the presence of $H_2O_2$ in the system

**Table 5** Experimental verification for succinic acid production from lignin depolymerization in $TiO_2$/UV with $H_2O_2$ in the system

| | % Yield of succinic acid | | |
| --- | --- | --- | --- |
| | **Actual** | **Predict** | **Error (%)** |
| 1 | 7.86 | 7.63 | 3.01 |
| 2 | 7.74 | 7.63 | 1.44 |
| 3 | 7.85 | 7.63 | 2.88 |

hydrogen peroxide level in the system could produce more hydroxyl radicals to break down lignin molecules into succinic acid. This result agrees with Ma et al.[11] and Yin et al [16], who indicated that hydroxyl radicals from hydrogen peroxide are crucial for depolymerization of lignin.

According to Box-Behnken design results, the optimum reaction conditions for the maximum %yield of succinic acid from lignin depolymerization under $TiO_2$/UV in the presence of $H_2O_2$ are found to be a reaction time of 24 h, $TiO_2$ dosage of 3 g/l and $H_2O_2$ dosage 25.45 µl, with a predicted %yield of succinic acid at 7.63%. Experiments were conducted under the optimized conditions with three replicates. The results showed that succinic acid yields were close to the predicted values shown in Table 5, indicating that this statistical approach is valid.

**4. Conclusions**

Lignin can be selectively depolymerized into dicarboxylic, acetic and succinic acids via a simple one-step process using $TiO_2$/UV in the presence of $H_2O_2$ without prior pH modification. Respond surface methodology (RSM) was conducted to study the interactions of three parameters, reaction time, $TiO_2$ dosage, and $H_2O_2$ dosage. A Box-Behnken design was used to optimize the %yield of succinic acid. The optimized parameters were found as a reaction time of 24 h., $TiO_2$ dosage of 3 g/l and $H_2O_2$ dosage of 25.45 µl. The predicted optimal % yield was close to the experimental value, 7.82%. These results suggest that dicarboxylic acid production from a renewable carbon source, such as lignin, is an attractive and environmentally friendly process due to its low chemical use. It is economically feasible due to its single-stage production.

**5. Acknowledgements**

**6. References**

[1] Schutyser W, Renders T, Van den Bosch S, Koelewijn SF, Beckham GT, Sels BF. Chemicals from lignin: an interplay of lignocellulose fractionation, depolymerisation, and upgrading. Chem Soc Rev. 2018;47(3):852-908.
[2] Zeng J, Yoo CG, Wang F, Pan X, Vermerris W, Tong Z. Biomimetic fenton-catalyzed lignin depolymerization to high-value aromatics and

dicarboxylic acids. Chem Sus Chem. 2015;8(5):861-71.

[3] Chen C, Jin D, Ouyang X, Zhao L, Qiu X, Wang F. Effect of structural characteristics on the depolymerization of lignin into phenolic monomers. Fuel. 2018;223:366-72.

[4] Deuss PJ, Barta K. From models to lignin: Transition metal catalysis for selective bond cleavage reactions. Coord Chem Rev. 2016;306:510-32.

[5] Fernández-Rodríguez J, Erdocia X, Sánchez C, González Alriols M, Labidi J. Lignin depolymerization for phenolic monomers production by sustainable processes. J Energ Chem. 2017;26(4):622-31.

[6] Bi Z, Li Z, Yan L. Catalytic oxidation of lignin to dicarboxylic acid over the CuFeS2 nanoparticle catalyst. Green Process Synth. 2018;7(4):306-15.

[7] Ma R, Guo M, Zhang X. Recent advances in oxidative valorization of lignin. Catal Today. 2018;302:50-60.

[8] Wang M, Ma J, Liu H, Luo N, Zhao Z, Wang F. Sustainable productions of organic acids and their derivatives from biomass via selective oxidative cleavage of C–C bond. ACS Catalysis. 2018;8(3):2129-65.

[9] Kang J, Irmak S, Wilkins M. Conversion of lignin into renewable carboxylic acid compounds by advanced oxidation processes. Renew Energ. 2019;135:951-62.

[10] Wang M, Zhang X, Li H, Lu J, Liu M, Wang F. Carbon modification of nickel catalyst for depolymerization of oxidized lignin to aromatics. ACS Catalysis. 2018;8(2):1614-20.

[11] Ma R., Guo M, Zhang X. Selective conversion of biorefinery lignin into dicarboxylic acids. Chem Sus Chem. 2014;7(2):412-5.

[12] Kamwilaisak K, Wright PC. Investigating laccase and titanium dioxide for lignin degradation. Energ Fuel. 2012;26(4):2400-6.

[13] Sun Z, Fridrich B, Santi A, Elangovan S, Barta K. Bright side of lignin depolymerization: toward new platform chemicals. Chem Rev. 2018;118(2):614-78.

[14] Wang JL, Xu LJ. Advanced oxidation processes for wastewater treatment: formation of hydroxyl radical and application. Crit Rev Environ Sci Tech. 2012;42(3):251-325.

[15] Cronin DJ, Zhang X, Bartley J, Doherty WOS. Lignin depolymerization to dicarboxylic acids with sodium percarbonate. ACS Sustain Chem Eng. 2017;5(7):6253-60.

[16] Yin G, Jin F, Yao G, Jing Z. Hydrothermal conversion of catechol into four-carbon dicarboxylic acids. Ind Eng Chem Res. 2015;54(1):68-75.

[17] Seesuriyachan P, Kuntiya A, Kawee-ai A, Techapun C, Chaiyaso T, Leksawasdi N. Improvement in efficiency of lignin degradation by Fenton reaction using synergistic catalytic action. Ecol Eng. 2015;85:283-7.

[18] Zhang D, Sun B, Duan L, Tao Y, Xu A, Li X. Photooxidation of guaiacol to organic acids with hydrogen peroxide by microwave discharge electrodeless lamps. Chem Eng Tech. 2016;39(1):97-101.

[19] Prado R, Erdocia X, Labidi J. Effect of the photocatalytic activity of TiO2 on lignin depolymerization. Chemosphere. 2013;91(9):1355-61.

[20] Tanaka K, Calanag R, Hisanaga T. Photocatalyzed degradation of lignin on TiO2. J Mol Catal Chem. 1999;138(2-3):287-94.

[21] Zhang H, Wang Z, Li R, Guo J, Li Y, Zhu J, et al. TiO2 supported on reed straw biochar as an adsorptive and photocatalytic composite for the efficient degradation of sulfamethoxazole in aqueous matrices. Chemosphere. 2017;185:351-60.

[22] Awungacha Lekelefac C, Busse N, Herrenbauer M, Czermak P. Photocatalytic based degradation processes of lignin derivatives. Int J Photoenergy. 2015;2015:1-18.

[23] Castellote M, Bengtsson N. Principles of TiO 2 photocatalysis, in applications of titanium dioxide photocatalysis to construction materials. In: Ohama Y, Van Gemert D, editors. Application of Titanium Dioxide Photocatalysis to Construction Materials. Berlin: Springer; 2011. p. 5-10.

[24] Liu C, Wu S, Zhang H, Xiao R. Catalytic oxidation of lignin to valuable biomass-based platform chemicals: a review. Fuel Process Tech. 2019;191:181-201.

[25] Ray S, Lalman JA. Using the box–benkhen design (BBD) to minimize the diameter of electrospun titanium dioxide nanofibers. Chem Eng J. 2011;169(1):116-25.

[26] Nam SN, Cho H, Han J, Her N, Yoon J. Photocatalytic degradation of acesulfame K: optimization using the box–behnken design (BBD). Process Saf Environ Protect. 2018;113:10-21.

[27] Tak BY, Tak BS, Kim YJ, Park YJ, Yoon YH, Min GH. Optimization of color and COD removal from livestock wastewater by electrocoagulation process: application of box–behnken design (BBD). J Ind Eng Chem. 2015;28:307-15.

[28] Schneider J, Matsuoka M, Takeuchi M, Zhang J, Horiuchi Y, Anpo M, et al. Understanding TiO2 photocatalysis: mechanisms and materials. Chem Rev. 2014;114(19):9919-86.

[29] Diantoro M, A Kusumaatmaja, Triyana K. Study on Photocatalytic properties of TiO2 nanoparticle in various pH condition. IOP Conf Series: Journal of Physics: Conf Series. 2018;1011:1-7.

[30] Tripathi A, Narayanan S. Impact of TiO2 and TiO2/g-C3N4 nanocomposite to treat industrial wastewater. Environ Nanotechnol Monit Manag. 2018;10:280-91.

[31] Zhu XD, Wang YJ, Sun RJ, Zhou DM. Photocatalytic degradation of tetracycline in aqueous solution by nanosized TiO2. Chemosphere. 2013;92(8):925-32.

[32] Safari GH, Hoseini M, Seyedsalehi M, Kamani H, Jaafari J, Mahvi AH. Photocatalytic degradation of tetracycline using nanosized titanium dioxide in aqueous solution. Int J Environ Sci Tech. 2015;12(2):603-16.

[33] Bazrafshan E, Al-Musawi TJ, Silva MF, Panahi AH, Havangi M, Mostafapur FK. Photocatalytic degradation of catechol using ZnO nanoparticles as catalyst: optimizing the experimental parameters using the box-behnken statistical methodology and kinetic studies. Microchem J. 2019;147:643-53.

[34] Zazouli MA, Balarak D, Mahdavi Y. Pyrocatechol removal from aqueous solutions by using azolla filiculoides. Health Scope. 2013;2(1):25-30.

[35] Dewidar H, Nosier S, El-Shazly A. Photocatalytic degradation of phenol solution using zinc oxide/uv. J Chem Health Saf. 2018;25(1):2-11.

[36] Hasegawa I, Inoue Y, Muranaka Y, Yasukawa T, Mae K. Selective production of organic acids and depolymerization of lignin by hydrothermal oxidation with diluted hydrogen peroxide. Energ Fuel. 2011;25(2):791-6.

[37] Li SH, Liu S, Colmenares JC, Xu YJ. A sustainable approach for lignin valorization by heterogeneous photocatalysis. Green Chem. 2016;18(3):594-607.

[38] Kansal S, Singh M, Sud D. Studies on TiO2/ZnO photocatalysed degradation of lignin. J Hazard Mater. 2008;153(1-2):412-7.

[39] Li X, Zou M, Wang Y. Soft-Template synthesis of mesoporous anatase TiO2 nanospheres and its enhanced photoactivity. Molecules. 2017;22(11): 1943.

[40] Saxena R, Saran S, Isar J, Kaushik R. Production and applications of succinic acid. In: Pandey A, Negi S, Soccol CR, editors. Current Developments in Biotechnology and Bioengineering. USA: Elsevier; 2017. p. 601-30.

[41] Li Q, Wang D, Wu Y, Li W, Zhang Y, Xing J, et al. One step recovery of succinic acid from fermentation broths by crystallization. Separ Purif Tech. 2010; 72(3):294-300.

[42] Nghiem NP, Kleff S, Schwegmann S. Succinic acid: technology development and commercialization. Ferment. 2017;3(2):1-14.

[43] Sadoun O, Rezgui F, G'Sell C. Optimization of valsartan encapsulation in biodegradables polyesters using Box-Behnken design. Mater Sci Eng C. 2018; 90:189-97.

[44] Shilpy M, Ehsan MA, Ali TH, Abd Hamid SB, Ali ME. Performance of cobalt titanate towards H 2 O 2 based catalytic oxidation of lignin model compound. RSC Adv. 2015;5(97):79644-53.